

# An Anionic Diplatinum DNA Photocleavage Agent: Chemical Mechanism and Footprinting of $\lambda$ Repressor

Klaus M. Breiner,<sup>†,‡</sup> Margaret A. Daugherty,<sup>§</sup> Terrence G. Oas,<sup>§</sup> and  
H. Holden Thorp<sup>\*,†</sup>

Contribution from the Department of Chemistry, University of North Carolina,  
Chapel Hill, North Carolina 27599-3290, and Department of Biochemistry,  
Duke University Medical Center, Durham, North Carolina 27710

Received July 26, 1995<sup>⊗</sup>

**Abstract:** The  $d\sigma^* \rightarrow p\sigma$  excited state of  $Pt_2(pop)_4^{4-}$  (**1**,  $pop = P_2O_5H_2^{2-}$ ) elicits frank scission of double-stranded DNA as assayed by high-resolution gel electrophoresis. The photoreaction of **1** and a 5'-<sup>32</sup>P-labeled 25-mer duplex produces a surprisingly even ladder of phosphate terminated bands with some modified bands that can be assigned as phosphoglycolate termini by comigration with the products of an  $Fe(EDTA)^{2-}/H_2O_2$  reaction. The analogous reaction of the 3'-<sup>32</sup>P-labeled duplex also produces phosphate termini and a modified band that can be assigned as a 5'-aldehyde terminus by  $NaBH_4$  reduction to the 5'-alcohol and comigration with authentic alcohol termini generated using alkaline phosphatase. These products are consistent with abstraction of the 4' and 5' hydrogens from the deoxyribose function; products indicative of 1' or 3' chemistry were not detected. The reaction is more efficient in the presence of  $O_2$ , which appears to trap the radical produced by homolytic C–H activation. The even cleavage ladder argues strongly against a  $^1O_2$  mechanism, and the cleavage is not enhanced in  $D_2O$ . Further, ethanol does not inhibit the reaction of **1** at concentrations up to 1 M, where the reaction of hydroxyl radical is completely quenched. These experiments point to a mechanism where the tetraanionic complex collides directly with the DNA to effect C–H activation, which is supported by a strong enhancement in cleavage by  $Mg^{2+}$ . This unusual reaction has been used to obtain a footprint of  $\lambda$  repressor bound to the  $O_R1$  sequence. The resolution of the footprint is similar to that of hydroxyl radical, which permits binding of the repressor to a single side of the DNA helix to be distinguished.

Chemical agents that cleave DNA by abstraction of sugar hydrogens can be used to observe distortions in nucleic acid structures from fluctuations in the cleavage pattern and to map of binding loci of transcription factors from footprinting experiments.<sup>1–3</sup> For reliable determination of footprints and structures, complete sequence neutrality of cleavage is desirable.<sup>4,5</sup> This goal has been achieved using the complex  $Fe(EDTA)^{2-}$ , which does not bind to DNA because of its dianionic charge and generates hydroxyl radical ( $\cdot OH$ ) upon treatment with hydrogen peroxide.<sup>1</sup> The  $\cdot OH$  is capable of abstracting all of the sugar hydrogens in the ribose function, which leads to strand scission.<sup>6</sup> Because  $\cdot OH$  is such a small species, intimate probing of the structure of nucleic acids or DNA–protein complexes is possible, allowing for imaging of subtle perturbations in the DNA structure and for high-resolution footprinting of DNA-binding proteins.<sup>7,8</sup>

We have developed a parallel approach to the  $Fe(EDTA)^{2-}/H_2O_2$  system based on the tetraanionic complex  $Pt_2(pop)_4^{4-}$  (**1**,

$pop = P_2O_5H_2^{2-}$ ).<sup>9,10</sup> This complex abstracts hydrogen atoms from organic substrates upon photolysis into the low-lying  $d\sigma^* \rightarrow p\sigma$  excited-state (367 nm, Scheme 1).<sup>11</sup> We reasoned that DNA photocleavage by **1** would exhibit an unusual dependence on the charge properties of the nucleic acid, especially if direct abstraction of hydrogen from DNA by **1**\* was responsible for strand scission. Furthermore, the absence of binding of **1** should provide a sequence-neutral footprint. Photolysis of **1** in the presence of DNA leads to nicking as assayed by plasmid electrophoresis.<sup>9</sup> Conversion of form I to form II plasmid by photolysis of **1** in phosphate buffer is accelerated at high ionic strength, and sodium formate, a  $\cdot OH$  scavenger, does not inhibit nicking. These observations point to a mechanism where **1**\* abstracts hydrogen atoms directly from DNA. Mononucleotides quench **1**\* with rate constants that are suggestive of 1'-hydrogen abstraction;<sup>10</sup> recent studies on oxoruthenium(IV) complexes suggest that abstraction of the 1'-hydrogen is the thermodynamically most facile pathway of sugar oxidation.<sup>12</sup>

We report here on the cleavage of double-stranded DNA oligomers by **1**\*. The cleavage reaction provides a surprisingly even ladder of cleavage bands that is similar to that obtained with  $Fe(EDTA)^{2-}$  and indicative of sugar oxidation as the sole reaction pathway. Oxygen must be present to realize strand scission, as expected for a cleavage agent that can only perform homolytic C–H activation to generate carbon-centered radicals.<sup>13</sup> The cleavage is quite efficient in the presence of  $Mg^{2+}$ , and electrophoresis gels show bands that can be confidently

<sup>†</sup> University of North Carolina.

<sup>‡</sup> Present address: Zentrum für Molekulare Biologie, Universität Heidelberg D-69120, Heidelberg, Germany.

<sup>§</sup> Duke University Medical Center.

<sup>⊗</sup> Abstract published in *Advance ACS Abstracts*, November 1, 1995.

(1) Pogozelski, W. K.; McNeese, T. J.; Tullius, T. D. *J. Am. Chem. Soc.* **1995**, *117*, 6428–6433.

(2) Tullius, T. D.; Dombroski, B. A.; Churchill, M. E. A.; Kam, L. *Meth. Enzymol.* **1987**, *155*, 537–558.

(3) Pyle, A. M.; Barton, J. K. *Prog. Inorg. Chem.* **1990**, *38*, 413.

(4) Mah, S. C.; Townsend, C. A.; Tullius, T. D. *Biochemistry* **1994**, *33*, 614–621.

(5) Sitlani, A.; Long, E. C.; Pyle, A. M.; Barton, J. K. *J. Am. Chem. Soc.* **1992**, *114*, 2303.

(6) Giese, B.; Dussy, A.; Elie, C.; Erdmann, P.; Schweiter, U. *Angew. Chem., Int. Ed. Engl.* **1994**, *33*, 1861–1862.

(7) Tullius, T. D.; Dombroski, B. A. *Proc. Natl. Acad. Sci. U.S.A.* **1986**, *83*, 5469–5473.

(8) Burkhoff, A. M.; Tullius, T. D. *Nature (London)* **1988**, *331*, 455.

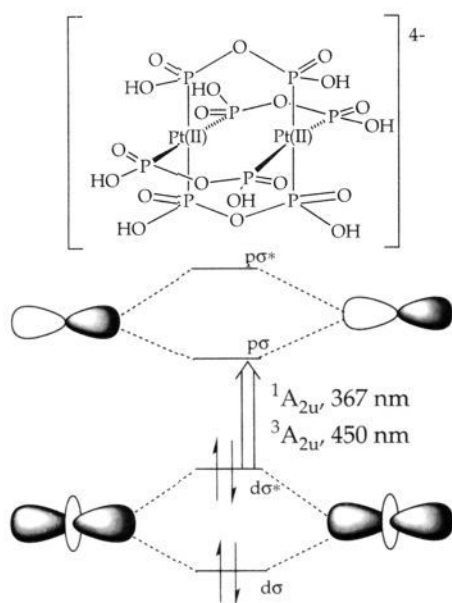
(9) Kalsbeck, W. A.; Grover, N.; Thorp, H. H. *Angew. Chem., Int. Ed. Engl.* **1991**, *30*, 1517.

(10) Kalsbeck, W. A.; Gingell, D. M.; Malinsky, J. E.; Thorp, H. H. *Inorg. Chem.* **1994**, *33*, 3313–3316.

(11) Roundhill, D. M.; Gray, H. B.; Che, C.-M. *Acc. Chem. Res.* **1989**, *22*, 55.

(12) Neyhart, G. A.; Cheng, C.-C.; Thorp, H. H. *J. Am. Chem. Soc.* **1995**, *117*, 1463–1471.

## Scheme 1



assigned by comigration to the termini expected for activation of the 4' and 5' hydrogens. We have applied this chemistry to obtaining the footprint of  $\lambda$  repressor<sup>14,15</sup> and find a footprint very similar to that obtained with  $\cdot\text{OH}$ .<sup>7</sup>

## Experimental Section

**Metal Complex.**  $\text{K}_4[\text{Pt}_2(\text{pop})_4]$  was prepared by a literature method.<sup>16</sup> Aqueous stock solutions were frozen in small aliquots, and the concentration was determined by UV absorbance,  $\epsilon(367 \text{ nm}) = 34\,500 \text{ M}^{-1} \text{ cm}^{-1}$ .<sup>16</sup>

**DNA Oligomers and Labeling.** All DNA concentrations throughout are given in terms of nucleotide phosphates. All DNA oligomers were acquired from the Oligonucleotide Synthesis Center in the Department of Pathology at UNC. Further purification was carried out as described previously.<sup>17</sup> Except for protein footprinting, all experiments were carried with a 25 bp duplex with the sequence (labeled strand): d[5'-(ATG GCG TAA TCA TGG TCA TAG CTG T)]. The oligomers used for footprinting experiments were purified by HPLC using a 15 cm column packed with SelfPack Poros 20 R2 (PerSeptive Biosystems) with a 0–20% gradient (buffer A, 50 mM triethylammonium acetate, 5% acetonitrile, buffer B, acetonitrile). The collected solutions were lyophilized to near dryness and twice precipitated with ethanol. The oligonucleotides were resuspended in MilliQ water, and concentrations were determined as described elsewhere.<sup>18</sup> Portions used for 5'- and 3'-labeling were additionally purified by 20% polyacrylamide gel electrophoresis. The homogeneous material was visualized with an UV hand lamp by placing the gel on a TLC F254 plate (Merck) and extracted as described.<sup>18</sup> The 5'-end-<sup>32</sup>P-labeled oligomer was prepared by using T4 polynucleotide kinase (New England Biolabs) and deoxyadenosine 5'-[ $\gamma$ -<sup>32</sup>P]-triphosphate (Amersham) as previously described.<sup>17</sup> The 3'-end-labeled oligomer was prepared in similar fashion using terminal deoxynucleotidyl transferase (Gibco BRL) and 2'-dideoxyadenosine 5'-[ $\alpha$ -<sup>32</sup>P]-triphosphate. Homogeneous 3'-labeled material was obtained by 20% polyacrylamide gel electrophoresis and extraction as described.<sup>18</sup> Annealing was performed by mixing the

complementary oligomers (8  $\mu\text{M}$ ), sodium phosphate buffer (20 mM, pH 7.0), and the labeled strand (30 000 cpm/20  $\mu\text{L}$ ); heating to 90  $^\circ\text{C}$  for 5 min; and slowly ( $\sim 2 \text{ h}$ ) cooling to room temperature. The formation of the duplex was confirmed by 20% polyacrylamide gel electrophoresis at 4  $^\circ\text{C}$ .

**Photocleavage Reactions.** Photolysis was performed in polyspring inserts (National Scientific Company) with a 300W Hg Lamp (Oriol) and a monochromator providing 368 nm (60% transmission, 40 nm FWHM). Typical final concentrations were 8  $\mu\text{M}$  DNA, 10 mM sodium phosphate buffer (pH 7.0), 5 mM  $\text{MgSO}_4$ , and 25  $\mu\text{M}$   $\text{K}_4[\text{Pt}_2(\text{pop})_4]$ ; the total volumes per lane were 40  $\mu\text{L}$ ; and the irradiation time was 10 min. Other specific conditions are given in the figure legends. After photolysis, purified<sup>18</sup> calf thymus DNA ( $\sim 1 \mu\text{g}$ ), 10  $\mu\text{L}$  of 1 M KCN, and 0.2 M EDTA were added to the samples, and the mixtures were incubated at 50  $^\circ\text{C}$  for 30 min to remove covalently attached Pt(II) resulting from the decomposition of **1** during photolysis. Ethanol precipitation, alkaline treatment with piperidine, and loading procedures were carried out as described.<sup>17</sup> Oxygen exclusion and saturation were obtained by lyophilizing the reaction mixtures to dryness in the reaction vials before sealing with a septum under an argon or oxygen flow through the septum. The volume was readjusted with MilliQ water that was thoroughly degassed (50 mL purged with nitrogen for 2 h with sonication for the first 1 h and 40 min) or saturated with oxygen. Control samples with and without platinum dimer were prepared identically, and the volumes were adjusted with untreated MilliQ water.

**Hydroxyl Radical Reactions.** All  $\text{Fe}(\text{EDTA})^{2-}$  reactions were carried out similar to literature methods.<sup>2</sup> In a typical reaction, 5  $\mu\text{L}$  each of ascorbate (8 mM),  $\text{Fe}(\text{EDTA})^{2-}$  (80  $\mu\text{M}$ ), and hydrogen peroxide (0.024%) were mixed at the wall of the vial containing 20  $\mu\text{L}$  of 8  $\mu\text{M}$  (bp) DNA with 30 000 cpm <sup>32</sup>P-label in 20 mM sodium phosphate (pH 7.0), and 5  $\mu\text{L}$  of MilliQ water or quencher solutions. The reaction was allowed to proceed for 5 min before quenching with 10  $\mu\text{L}$  of 0.1 M thiourea and 1  $\mu\text{L}$  of 0.2 M EDTA. The DNA was recovered by ethanol precipitation as in the photocleavage reactions.

**Fragment Modifications.**  $\text{NaBH}_4$  reduction was achieved by resuspending the precipitate in 40  $\mu\text{L}$  of 0.2 M  $\text{NaBH}_4$  solution. The reaction proceeded for 15 min at room temperature upon quenching with 2 equiv. of acetic acid (8  $\mu\text{L}$ , 1 M) followed by ethanol precipitation, as described above. The removal of the 5'-phosphate from the fragments after the photolysis reaction and piperidine treatment was achieved by treating the resuspended pellet with 10 units of calf intestinal alkaline phosphatase (Promega) for 30 min at 37  $^\circ\text{C}$  (total volume 50  $\mu\text{L}$ ).

**Footprinting of  $\lambda$  Repressor.** The protein footprinting experiment was carried out with a 39 bp oligomer containing the  $\lambda$  repressor binding sequence  $O_{R1}$ ; only the coding strand was labeled: d(GTT GAC TAT TTT ACC TCT GGC GGT GAT AAT GGT TGC ATG). Repressor protein was purified from the bacterial strain, *E. coli* X90, containing the plasmid pRB200 (expressing full length repressor protein under the control of the Ptac promoter; a generous gift of Robert Sauer) using the procedure of Johnson et al.<sup>19</sup> with the modifications described by Brenowitz et al.<sup>20</sup> Repressor was dialyzed extensively against 10 mM Tris-Cl, pH 8.0, 2 mM  $\text{CaCl}_2$ , 0.1 mM  $\text{Na}_2\text{EDTA}$ , 0.1 mM DTT, 5% glycerol, and 200 mM KCl and stored frozen until use. Total monomer concentration was determined assuming an  $\epsilon(280 \text{ nm}) = 1.18 \text{ mL/cm} \cdot \text{mg}$ .<sup>21</sup>

The footprinting reactions were carried out as described above in a total volume of 40  $\mu\text{L}$  with 10 nM 39 mer duplex and 0.25–2  $\mu\text{M}$  protein. The blank reaction was carried out with half concentration of platinum dimer. Photolysis and workup were as described above. Saturation of protein in the binding site was confirmed with a mobility shift assay of the reaction mixture using 10% polyacrylamide gel electrophoresis under native conditions (100 V, 4  $^\circ\text{C}$ ).

**Electrophoresis.** The DNA fragments were analyzed using 20% polyacrylamide (19:1 acrylamide:bisacrylamide) gel electrophoresis under denaturing conditions (7 M urea). Electrophoresis was usually performed at 15 W constant power. Cleavage bands were visualized

(13) Stubbe, J.; Kozarich, J. W. *Chem. Rev.* **1987**, *87*, 1107.

(14) Jordan, S. R.; Pabo, C. O. *Science* **1988**, *242*, 893–899.

(15) Sauer, R. T.; Hehir, K.; Stearman, R. S.; Weiss, M. A.; Jeitler-Nilsson, A.; Suchanek, E. G.; Pabo, C. O. *Biochemistry* **1986**, *25*, 5992–5998.

(16) Che, C. M.; Butler, L. G.; Grunthaner, P. J.; Gray, H. B. *Inorg. Chem.* **1985**, *24*, 4662.

(17) Cheng, C.-C.; Goll, J. G.; Neyhart, G. A.; Welch, T. W.; Singh, P.; Thorp, H. H. *J. Am. Chem. Soc.* **1995**, *117*, 2970–2980.

(18) Maniatis, T.; Fritsch, E. F.; Sambrook, J. *Molecular Cloning: A Laboratory Manual*; 2nd ed.; Cold Spring Harbor Press: 1989.

(19) Johnson, A. D.; Pabo, C. O.; Sauer, R. T. *Methods Enzymol.* **1985**, *65*, 839–856.

(20) Brenowitz, M.; Senear, D. F.; Shea, M. A.; Ackers, G. K. *Methods Enzymol.* **1986**, *130*, 132–181.

(21) Sauer, R. T.; Andregg, R. *Biochemistry* **1978**, *17*, 1092–1100.

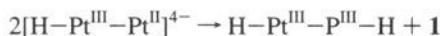
using Fuji RX, Kodak X-Omat Ar-5, and Kodak BioMax MR at  $-78^{\circ}\text{C}$  for 10–24 h. The quantitation of cleavage was performed with an Apple OneScanner and the NIH Image program. Care was taken to insure that saturation of the film did not occur and that densitometry gave a Gaussian peak, as shown in Figure 6.

## Results

**Photochemistry of DNA Cleavage.** The photophysics of **1** are dominated by the Pt–Pt interaction, which leads to filled  $d\sigma$  and  $d\sigma^*$  levels as shown in Scheme 1.<sup>11</sup> As a result, the formal bond order in the ground state is zero. Excitation of a  $d\sigma^*$  electron into the  $\sigma$  bonding level formed from the higher lying  $p_z$  orbitals leads to a formal Pt–Pt bond order of 1 in the excited state. This excited state is capable of abstracting hydrogen atoms from a variety of organic and organometallic substrates to form a hydrido Pt(III,II) dimer.<sup>22,23</sup>



The Pt(III,II) species then disproportionates to **1** and a Pt(III,-III) dihydrido complex



The Pt(III,III) complex can then photochemically eliminate  $\text{H}_2$  to regenerate **1** and complete a photocatalytic cycle. In aqueous solution, hydrolysis of the pop ligands leads to catalyst deactivation;<sup>24</sup> however, we have demonstrated that the catalytic cycle is efficient enough to realize 100 turnovers for oxidation of 1-phenylethanol to acetophenone.<sup>10</sup>

The radical mechanism for oxidation of organic substrates by **1**<sup>\*</sup> implies that cleavage of DNA might also proceed by hydrogen abstraction. The rate constants for quenching of **1**<sup>\*</sup> by nucleotide monophosphates are  $\sim 10^5 \text{ M}^{-1} \text{ s}^{-1}$ ,<sup>10</sup> similar to those for alcohols with similar C–H bond strengths.<sup>11</sup> Oxidation of guanine nucleotides is not enhanced relative to the other nucleotides, implying that base oxidation pathways are unimportant.<sup>12</sup> Further, the oxidation of the nucleotides is faster than the simple sugars, and oxidation of deoxynucleotides is faster than oxidation of ribonucleotides. As discussed in detail elsewhere, these observations are consistent with abstraction of the 1'-hydrogen, which is accelerated by the adjacent aromatic base but attenuated by the polar effect of the 2'-hydroxyl.<sup>12</sup> In the nucleotides, it is likely that the 1' position is the thermodynamically most facile to activate,<sup>25</sup> so **1**<sup>\*</sup> may select on the basis of reactivity in the mononucleotides where a folded structure does not prohibit reaction of individual hydrogens.

Photolysis of **1** in the presence of a synthetic 5'-<sup>32</sup>P-labeled double-stranded oligomer leads to surprisingly sequence-neutral cleavage as visualized by high-resolution gel electrophoresis (Figure 1). Comigration with a Maxam–Gilbert sequencing lane shows that the primary bands are phosphate-terminated and are enhanced by piperidine treatment. Shown in Figure 1 are results for photolysis solutions that are  $\text{N}_2$ -purged (lane 5), ambient  $\text{O}_2$  concentration (lane 4), and  $\text{O}_2$ -saturated (lane 3). The presence of  $\text{O}_2$  clearly leads to higher extents of scission, and the increase in cleavage induced by  $\text{O}_2$  is the same at all sites. As discussed earlier,<sup>9</sup> photolysis in the degassed solution still leads to nicking as observed in the plasmid assay. This result could be attributed to trace  $\text{O}_2$  or to scission of the 4'

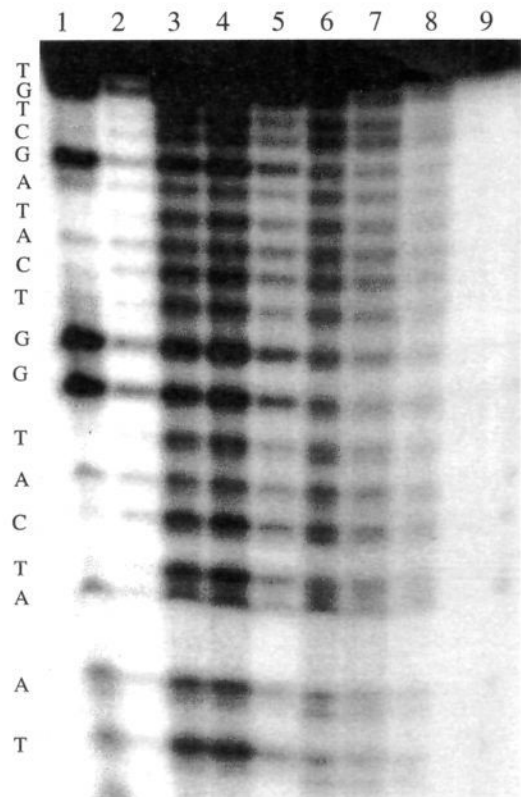


**Figure 1.** Autoradiogram of a polyacrylamide gel showing oxidation of 5'-labeled 25-mer duplex by **1** ( $200 \mu\text{M}$ ) in the absence of  $\text{Mg}^{2+}$ . Lane 1, Maxam–Gilbert reaction; lane 2, DNA photolyzed and treated with piperidine ( $90^{\circ}\text{C}$ , 30 min); lane 3, DNA photolyzed with **1** under oxygen saturation and treated with piperidine; lane 4, DNA photolyzed with **1** at ambient conditions and treated with piperidine; lane 5, DNA photolyzed with **1** under nitrogen degassed conditions and treated with piperidine. Lanes 6–9 correspond to lanes 3, 4, 5, and 2, respectively, without piperidine treatment. All other concentrations are given in the Experimental Section.

radical itself, which has been demonstrated.<sup>6</sup> Further, a mechanism involving sensitization of singlet oxygen by **1**<sup>\*</sup> is not likely, since DNA cleavage by  $^1\text{O}_2$  is specific for guanine base oxidation<sup>26</sup> and would not be expected to yield the even ladders shown in Figure 1. Furthermore, the extent of cleavage is not enhanced in  $\text{D}_2\text{O}$  as would be expected for a singlet oxygen mechanism. Previous plasmid studies showed that nicking was not inhibited by the  $\bullet\text{OH}$  scavenger sodium formate; the experiment in Figure 1 was repeated with increasing (0.1 mM–1 M) concentrations of ethanol, which had no effect on the cleavage intensities (gel shown in supporting information) but dramatically inhibited cleavage by  $\text{Fe}(\text{EDTA})^{2-}$ , as discussed elsewhere.<sup>2</sup>

Some piperidine-enhanced cleavage is apparent at the guanine residues in Figure 1. This reaction could arise from C–H activation in the guanine nucleobase, such as abstraction of the C8 hydrogen to make 8-oxoguanine, which gives a piperidine labile lesion.<sup>27,28</sup> Alternatively, **1**<sup>\*</sup> should be a strong enough one-electron oxidant<sup>29</sup> to abstract an electron from guanine. The guanine radical cation is known to react with water to form 8-oxoguanine and produce piperidine-labile lesions.<sup>30–32</sup>

(22) Roundhill, M. D.; Atherton, S. J.; Shen, Z. P. *J. Am. Chem. Soc.* **1987**, *109*, 6076.

(23) Harvey, E. L.; Stiegman, A. E.; Vlcek, A. A.; Gray, H. B. *J. Am. Chem. Soc.* **1987**, *109*, 5233.

(24) Bryan, S. A.; Dickson, M. K.; Roundhill, M. D. *Inorg. Chem.* **1987**, *26*, 3878.

(25) Miasiewicz, K.; Osman, R. *J. Am. Chem. Soc.* **1994**, *116*, 232–238.

(26) Fleisher, M. B.; Waterman, K. C.; Turro, N. J.; Barton, J. K. *Inorg. Chem.* **1986**, *25*, 3549–3551.

(27) Burrows, C. J.; Rokita, S. E. *Acc. Chem. Res.* **1994**, *27*, 295–301.

(28) Chen, X.; Burrows, C. J.; Rokita, S. E. *J. Am. Chem. Soc.* **1991**, *113*, 5884.

(29) Roundhill, M. D. *J. Am. Chem. Soc.* **1985**, *107*, 4354.

An intriguing observation from the initial plasmid studies centered on the effect of ionic strength on the cleavage intensities,<sup>9</sup> which has also been exploited in using quenching of unbound **1**\* to determine binding constants of exogenous metal complex quenchers.<sup>33</sup> In potassium phosphate buffer, increasing ionic strength leads to greater cleavage as determined in the plasmid assay. Most cationic cleavage agents that bind to DNA prior to effecting strand scission are accelerated at low ionic strength where electrostatic interactions are maximized<sup>34</sup> and cleavage by  $\text{Fe}(\text{EDTA})^{2-}/\text{OH}$  is independent of ionic strength.<sup>1,35</sup> The observation of increasing reaction with increasing ionic strength therefore supports the idea that strand scission occurs via direct reaction of **1**\* with the DNA and is not mediated by a diffusible intermediate. In the cleavage of the double-stranded oligomer from Figure 1, detection of increased cleavage by increased monovalent cation concentration is difficult because of the lower sensitivity to individual cleavage events of the double-stranded scission compared to the plasmid assay. However, a dramatic enhancement of cleavage is observed following addition of  $\text{Mg}^{2+}$  to the buffer (gel given in supporting information). The overall cleavage intensity increases with increasing  $[\text{Mg}^{2+}]$ , and a 20-fold increase in intensity is realized at 5 mM  $\text{Mg}^{2+}$ . A similar effect on plasmid nicking was observed with  $\text{Zn}^{2+}$ .

**Cleavage Termini and Sugar Oxidation Mechanism.** As shown in Figure 1, cleavage of the 5'-labeled oligomer provides primarily phosphate termini. A higher resolution gel is given in Figure 2, which shows that a second, faster-moving band is also obtained (lanes 1 and 2). For comparison, a reaction of  $\text{Fe}(\text{EDTA})^{2-}/\text{H}_2\text{O}_2$  is also shown in lanes 3 and 4. There is a striking resemblance between the  $\text{Fe}(\text{EDTA})^{2-}$  and **1**\* cleavage patterns both in the even ladders produced and in the presence of the same faster-moving band in both reactions. Experiments on  $\text{Fe}(\text{EDTA})^{2-}$  and iron bleomycin have demonstrated that this faster-moving band corresponds to the 3'-phosphoglycolate (**2**) obtained from activation of the 4' position of the sugar (relevant mechanisms are shown in Scheme 2).<sup>1,13,36,37</sup> Piperidine treatment enhances the intensity of the phosphate termini but not the 3'-phosphoglycolate (lane 2), which is also consistent with oxidation at the 4' position. Studies on octahedral rhodium(III) photocleavage agents have demonstrated a 3'-phosphoglycaldehyde (**5**) derived from 3' oxidation.<sup>5</sup> To eliminate the presence of this terminus in the reactions of **1**\*, the reaction mixtures from Figure 3 were treated with  $\text{NaBH}_4$ , which reduces the 3-phosphoglycaldehyde to the corresponding alcohol. No change in the phosphate and phosphoglycolate bands was observed in the reaction of **1**\*, although a new band did appear in the  $\text{Fe}(\text{EDTA})^{2-}$  reaction (gel given in supporting information). The slower-moving band corresponding to the 3'-furenone terminus derived from activation of the 1'-position (**4**) was also not observed.<sup>17,38,39</sup> Results on the 5'-labeled fragment therefore

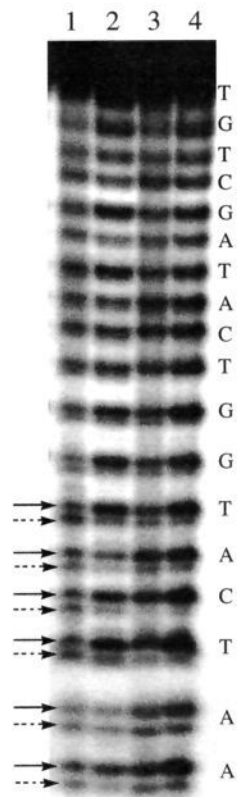
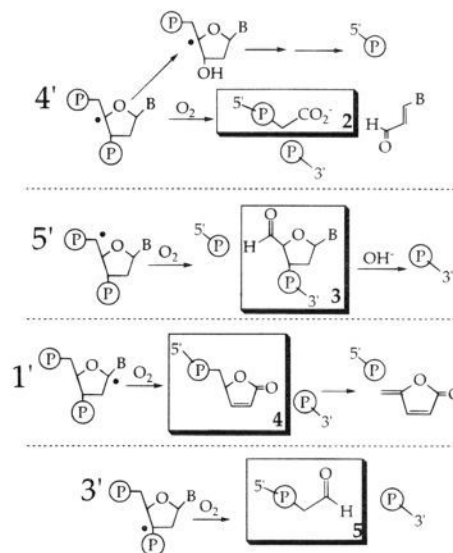


**Figure 2.** Autoradiogram of a polyacrylamide gel showing oxidation of the 5'-labeled 25-mer duplex by **1** and  $\text{Fe}(\text{EDTA})^{2-}/\text{H}_2\text{O}_2$ . Lane 1, DNA photolyzed with **1**; lane 2, DNA photolyzed with **1** and treated with piperidine; lane 3, DNA treated with  $\text{Fe}(\text{EDTA})^{2-}$  and  $\text{H}_2\text{O}_2$ ; lane 4, lane 3 + piperidine treatment. Conditions of  $\text{Fe}(\text{EDTA})^{2-}$  reaction are given in the Experimental Section.

### Scheme 2



support oxidation at the 4' position and do not support significant amounts of oxidation at 3' or 1'.

Cleavage by **1**\* was also performed on the 3'-<sup>32</sup>P-labeled double-stranded oligomer. As in the 5'-labeled case, the primary terminus obtained was the 5'-phosphate (Figure 3), which comigrated with the Maxam–Gilbert reaction. Prior to piperidine treatment, a second band was apparent and is indicated with the solid arrows (lane 2). This product disappeared upon treatment with piperidine. A reasonable explanation for this

(30) Kasai, H.; Yamgizumi, Z.; Berger, M.; Cadet, J. *J. Am. Chem. Soc.* **1992**, *114*, 9692.

(31) Johnston, D. H.; Glasgow, K. C.; Thorp, H. H. *J. Am. Chem. Soc.* **1995**, *117*, 8933–8937.

(32) Johnston, D. H.; Cheng, C.-C.; Campbell, K. J.; Thorp, H. H. *Inorg. Chem.* **1994**, *33*, 6388–6390.

(33) Kalsbeck, W. A.; Thorp, H. H. *J. Am. Chem. Soc.* **1993**, *115*, 7146–7151.

(34) Manning, G. S. *Acc. Chem. Res.* **1979**, *12*, 443.

(35) Lu, M.; Guo, Q.; Wink, D. J.; Kallenbach, N. R. *Nucleic Acids Res.* **1990**, *18*, 3333–3337.

(36) Pratviel, G.; Bernadou, J.; Meunier, B. *Angew. Chem., Int. Ed. Engl.* **1995**, *34*, 746–769.

(37) Hecht, S. M. *Acc. Chem. Res.* **1986**, *19*, 83.

(38) Goynes, T. E.; Sigman, D. S. *J. Am. Chem. Soc.* **1987**, *109*, 2846.

(39) Pitić, M.; Bernadou, J.; Meunier, B. *J. Am. Chem. Soc.* **1995**, *117*, 2935–2936.

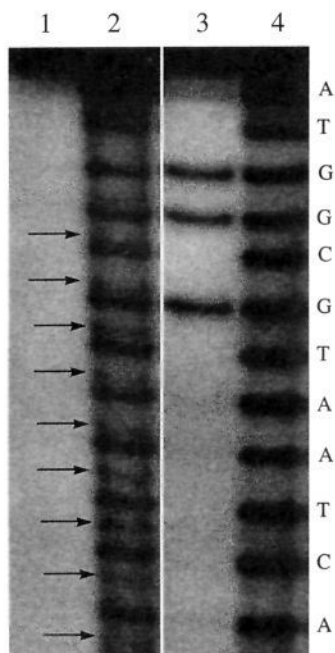
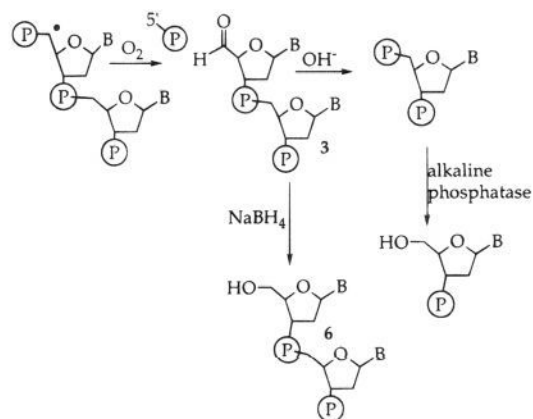


**Figure 3.** Autoradiogram of a polyacrylamide gel showing oxidation of the 3'-labeled 25-mer duplex by **1**. Lane 1, photolyzed DNA; lane 2, DNA photolyzed with **1**; lane 3, Maxam-Gilbert G lane; lane 4, lane 2 + piperidine treatment.

### Scheme 3



new band is the formation of the 5'-aldehyde (**3**) that can be derived from abstraction of the 5' hydrogen.<sup>36</sup> Piperidine treatment would be expected to hydrolyze this terminus to the 5'-phosphate.

To confirm that the second band in the 3'-labeled fragment corresponded to **3**, the cleavage reactions were treated with NaBH<sub>4</sub>, which converts the 5'-aldehyde to the 5'-alcohol (Scheme 3, **6**).<sup>40</sup> Treatment with NaBH<sub>4</sub> did in fact convert the putative 5'-aldehyde band (lane 1, arrows) to a slower-moving band (lane 2, arrows) (Figure 4). To confirm that this band was in fact the 5'-alcohol, the reaction mixture was treated with piperidine to form primarily phosphate termini (lane 4) and was then treated with alkaline phosphatase to remove the 5'-phosphate and generate the 5'-alcohol. These authentic 5'-alcohols (lane 3) did in fact comigrate with the bands derived from NaBH<sub>4</sub> reduction of the **1**\* cleavage product (arrows, lane 2).

**Footprinting of  $\lambda$  Repressor.** The  $\lambda$  repressor protein binds to double-stranded DNA at the O<sub>R</sub>1 operator sequence.<sup>14,15</sup> The binding locus of the dimer of  $\lambda$  repressor has been determined by footprinting with  $\cdot\text{OH}^7$  and other chemical nucleases,<sup>2</sup> and

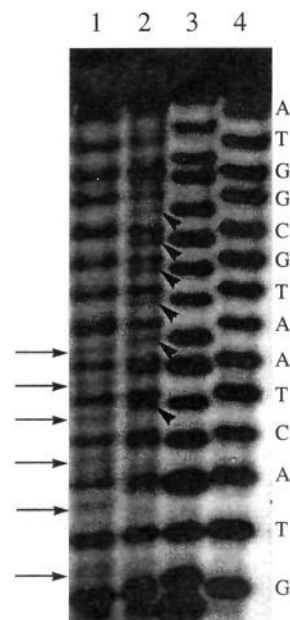


**Figure 4.** Autoradiogram of a polyacrylamide gel showing oxidation of the 3'-labeled 25-mer duplex by **1**. Lane 1, DNA photolyzed with **1**; lane 2, lane 1 + NaBH<sub>4</sub>; lane 3, lane 1 + piperidine treatment + alkaline phosphatase; lane 4, lane 1 + piperidine treatment.

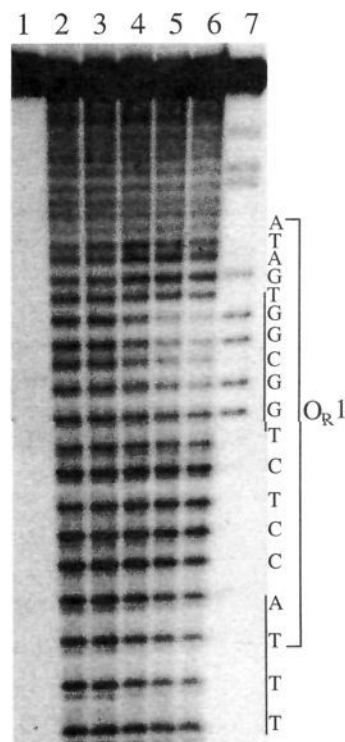


**Figure 5.** Polyacrylamide gel showing the footprinting of  $\lambda$  repressor by **1**. Lane 1, DNA photolyzed; lane 2, DNA photolyzed with **1**; lanes 3-6, DNA photolyzed with **1** and  $\lambda$  repressor (0.25, 0.5, 1, and 2  $\mu\text{M}$ , respectively); lane 7, Maxam-Gilbert G reaction. The O<sub>R</sub>1 sequence is labeled at right.

an X-ray crystal structure of the DNA-binding domain bound to the operator is also available.<sup>7</sup> A double-stranded oligomer containing O<sub>R</sub>1 and 11 bp on either side was synthesized and labeled at the 5' end of the coding strand. As shown in Figure 5, photolysis of this fragment in the presence of **1** leads to the even cleavage ladder obtained with the other oligomer (lane 2). The cleavage reaction was repeated in the presence of the

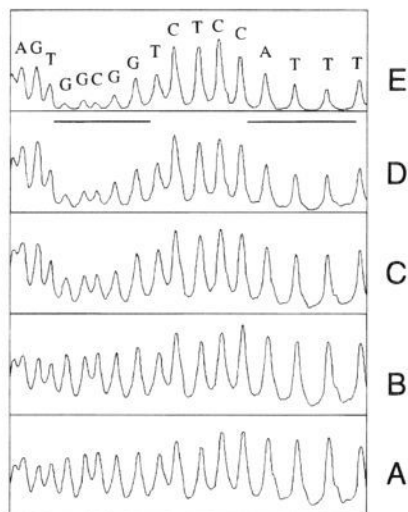


**Figure 6.** Densitometry from Figure 5 of (A) lane 2, (B) lane 3, (C) lane 4, (D) lane 5, and (E) lane 6.

$\lambda$  repressor under conditions where a mobility shift assay showed substantial binding of DNA to the protein. Binding of the protein protects two regions from cleavage by **1**\* at 5'-TTA and 5'-GCGG (lane 1, bars). The footprint is very similar to that obtained using  $\text{Fe}(\text{EDTA})^{2-}$  and  $\text{H}_2\text{O}_2$ .<sup>7</sup> The results are consistent with the crystal structure of the DNA-protein complex;<sup>14</sup> although the  $\lambda$  repressor resides in the major groove in the binding site, the strands that contact the protein are protected on both the major and minor groove sides.

The similarity of the footprints for **1**\* and  $\text{Fe}(\text{EDTA})^{2-}$  is emphasized by densitometry on the footprinting reaction (Figure 6). The primary protection of the three bases in the 5'-TTA half-site with some protection of the T and C on either side is nearly identical to that observed for  $\text{Fe}(\text{EDTA})^{2-}$  footprinting (note that the  $\text{Fe}(\text{EDTA})^{2-}$  footprint was performed with 3' labeling on the coding strand).<sup>7</sup> In the other half-site, the transition observed at the 5'-GT step is also seen in the  $\text{Fe}(\text{EDTA})^{2-}$  footprint, and the degree of protection at either side of the site is very similar. The most important feature that the two footprints have in common is the protection of two discrete half-sites with no protection in between, showing that the repressor binds only to one side of the DNA helix. In the DNaseI, Cu-phenanthroline, and MPE·Fe(II) footprints, the entire region is protected, which does not permit binding of the protein to a single side of the helix to be distinguished.<sup>2</sup>

## Discussion

**Chemical Mechanism.** A number of important points arise from the studies of the chemical mechanism. In recent studies on oxoruthenium(IV) complexes, we have shown that abstraction occurs from the 1' position in both mononucleotides and DNA.<sup>12,17</sup> This correspondence probably arises because the 1' position is the weakest C-H bond, and the oxoruthenium(IV) oxidant is tuned thermodynamically so that only activation of the weakest bond occurs, regardless of the DNA structure. In duplex DNA, the 1' hydrogen is much deeper in the groove than the 4' or 5' hydrogens; however, complexes that bind to DNA can access the 1' position.<sup>36</sup> Previous quenching studies on **1** with mononucleotides imply that abstraction also occurs primarily from the 1' position.<sup>10</sup> However, the studies described here show clearly that abstraction occurs only from the 4' and 5' positions in duplex DNA. Apparently, the electrostatic repulsions between the polyanion and the tetraanionic complex direct the oxidant toward the more accessible hydrogens.

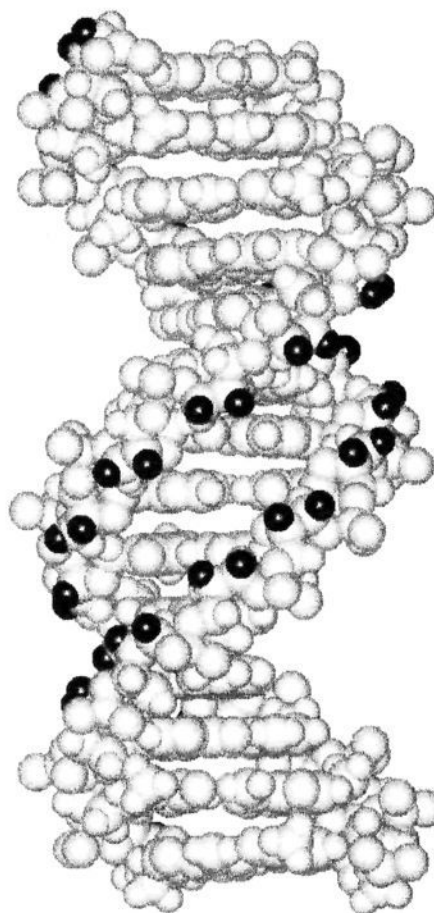


**Figure 7.** Structure of the B-DNA helix with the 4' and 5' hydrogens, which line the edge of the minor groove, shown in black.

Because of its high reactivity, electrical neutrality, and small size, it seems likely that the chemical mechanism of  $\cdot\text{OH}$  cleavage will involve the activation of more than just the 4' and 5' C-H bonds, and the  $\text{NaBH}_4$  reduction experiment discussed here provides some qualitative evidence in support of abstraction of at least the 3' hydrogen.

From electrostatic considerations,<sup>41</sup> targeting of the 3'-hydrogen by the anionic **1** might be expected, because the 3'-hydrogen resides in the major groove where the negative charge density is much lower.<sup>36</sup> The 4' and 5' hydrogens are located close to the phosphates and in the minor groove where the negative charge density is much higher (Figure 7). One explanation might be that although the 4' and 5' hydrogens are in the minor groove, the overall solvent accessibility is higher than for the 3' hydrogen. Another factor may lie in the observed impact of divalent cations, particularly  $\text{Mg}^{2+}$ , which greatly increase the cleavage efficiency. The buffer cations certainly reside primarily in the minor groove, so if the divalent cations bridge between **1** and DNA, the cleavage agent could be directed toward the minor groove. The pyrophosphite oxygens from **1** could coordinate to  $\text{Mg}^{2+}$ , which would facilitate the interaction.

**Footprinting.** Footprinting with enzymes and chemical nucleases provides qualitative information on binding modes and loci as well as thermodynamic information on binding affinities in solution.<sup>42,43</sup> Imaging of the structures of DNA and DNA-protein complexes with  $\cdot\text{OH}$  generated by the  $\text{Fe}(\text{EDTA})^{2-}/\text{H}_2\text{O}_2$  reaction has been extremely successful and can be performed on small quantities of material sufficient only for detection by radiolabeling.<sup>1,2,44</sup> The system discussed here provides a new alternative approach that may be advantageous

in certain situations. Photoreactions of **1** provide a high-resolution footprint where binding of  $\lambda$  repressor to a single side of the DNA helix can be discerned, which was obtained previously only with  $\cdot\text{OH}$ .<sup>7</sup> DNA cleavage by **1\*** is not quenched by alcohol; glycerol is a common component of some protein preparations and does quench the  $\cdot\text{OH}$  reaction.<sup>2</sup> When alcohol is present, **1\*** offers a distinct advantage over  $\cdot\text{OH}$  for high-resolution footprinting.

Photocatalysis with **1** in aqueous solution leads to catalyst decomposition through hydrolysis of the pyrophosphito ligand, resulting in mononuclear Pt(II) products.<sup>10</sup> For activation of organic substrates, up to 100 turnovers have been realized under favorable conditions. This decomposition offers advantages and disadvantages for implementation of the assay. The decomposition simplifies the tuning of conditions to obtain an acceptable ladder, because the intensity and time can simply be adjusted so that photolysis is continued until all of the catalyst is consumed, which can be monitored visually via the intense green emission of **1**. We have used a variety of light sources, including a readily available tanning lamp, to achieve these conditions. The only adjustable parameter is then the concentration of **1**, which can be readily determined for stable aqueous stock solutions from the absorption spectrum. The disadvantage is that the mononuclear Pt(II) compounds generated bind covalently to the DNA and must be removed by treatment with  $\text{CN}^-$ . Besides adding a step to the workup, this treatment could interfere with the assay. For example, we have observed that  $\text{CN}^-$  treatment hydrolyzes RNA, so an alternative treatment must be found if **1\*** is to be used to image RNA.

Another attractive feature apparent in the results here is that the extent of 4' and 5' chemistry can be readily assessed from the electrophoresis results. At sufficiently high resolution, it is possible to observe the phosphoglycolate band in the 5'-labeled fragment, which is indicative of 4' abstraction,<sup>1</sup> and the modified aldehyde band in the 3'-labeled fragment, which is indicative of 5' abstraction.<sup>40</sup> Quantitative assessment of these modified termini may permit the resolution of the footprints to be extended to protection of individual hydrogens by the protein.

The similarity of the footprints of **1\*** and  $\cdot\text{OH}$  is somewhat surprising, because  $\cdot\text{OH}$  is small and electrically neutral, while

**1\*** is a bulky anion. Nevertheless, the results clearly show that the same sites are protected from both reagents to similar extents by binding of the protein. The differences in the chemical mechanisms also do not alter the footprint. It therefore appears that the lack of binding of the reagent is of primary importance and that **1\*** is small enough to provide high resolution. Furthermore, the results show that the approach of the tetraanionic **1\*** against the electrostatic repulsion of the polyanionic DNA is not sufficient to prohibit efficient reaction and high-resolution footprinting. This feature may ultimately provide a means for probing the effects of electrostatic forces in the binding of proteins and small molecules to nucleic acids.<sup>41,45,46</sup>

**Acknowledgment.** We thank Professor Tom Tullius and his group for helpful discussions and Professor Robert Sauer for sharing his  $\lambda$  repressor plasmids. K.M.B. thanks the Konrad Adenauer Foundation for a fellowship. H.H.T. thanks the David and Lucile Packard Foundation and the National Science Foundation for support. The work of T.G.O. is supported by grants from the American Cancer Society (JFRA-398) and National Institutes of Health (GM45322).

**Supporting Information Available:** Gels showing the effects of ethanol,  $\text{Mg}^{2+}$ , and  $\text{NaBH}_4$  (3 pages). This material is contained in many libraries on microfiche, immediately follows this article in the microfilm version of the journal, can be ordered from the ACS, and can be downloaded from the Internet; see any current masthead page for ordering information and Internet access instructions.

JA952514H

(40) Pratiel, G.; Duarte, V.; Bernadou, J.; Meunier, B. *J. Am. Chem. Soc.* **1993**, *115*, 7939–7943.

(41) Jayaram, B.; Sharp, K. A.; Honig, B. *Biopolymers* **1989**, *28*, 975–993.

(42) Koblan, K. S.; Ackers, G. K. *Biochemistry* **1992**, *31*, 57–65.

(43) Merabet, E.; Ackers, G. K. *Biochemistry* **1995**, *34*, 8554–8563.

(44) Dixon, W. J.; Hayes, J. J.; Levin, J. R.; Weidner, M. F.; Dombroski, B. A.; Tullius, T. D. *Methods Enzymol.* **1991**, *208*, 380–413.

(45) Honig, B.; Nicholls, A. *Science* **1995**, *268*, 1144–1149.

(46) Sharp, K. A.; Honig, B.; Harvey, S. C. *Biochemistry* **1990**, *29*, 340–346.